JOURNAL OF OPTOELECTRONICS AND ADVANCED MATERIALS Vol. 22, No. 1-2, January – February 2020, p. 17 - 22

Generation and propagation properties of spatiotemporal necklace-ring solitons in the Ginzburg-Landau equation with an umbrella-shaped potential

GUANGYU JIANG*, KEJUN ZHONG, TIANYI XU
Key Laboratory of Nondestructive Testing, Ministry of Education, Nanchang Hangkong University, Nanchang 330063, China

We investigate the generation and propagation properties of spatiotemporal necklace-ring solitons(NRSs) from the vortex with the topological charges in three-dimensional complex Ginzburg-Landau equation (3D-CGLE) with an umbrella-shaped potential (USP).Under the action of the umbrella-shaped potential, the evolution dynamics of spatiotemporal necklace-ring solitons are studied comprehensively and thoroughly. The formation of spatiotemporal necklace-ring solitons does not only depend on the umbrella-shaped potential but also transmission properties. As the appropriate potential and its parameters are given, the vortices with *S*=2 can evolve the spatiotemporal necklace-ring solitons more easily than these with *S*=1 on the same propagation distance. The results suggest potential applications in optical communication devices and nonlinear dissipative media.

(Received February 26, 2019; accepted February 17, 2020)

Keywords: Nonlinear optics, Necklace-ring solitons, Ginzburg-Landau equation

1. Introduction

Complex Ginzburg-Landau equations (CGLE) have been widely used in physics and applied mathematics communities as a class of universal models with many applications for nonlinear optics, fluid dynamics, and chemical waves to second-order phase transitions, including superfluidity, superconductivity, liquid crystals, Bose-Einstein condensates and quantum field theories [1-7]. Recently, a lot of works mainly focus on cubic-quintic complex Ginzburg-Landau equations, which localize more complex patterns in optical media, such as dissipative spatial solitons, vortex solitons, necklace-ring solitons [8-19] etc. A. Barthelemy et al observed firstly that the necklace-ring beams could exist stably in Kerr medium and investigated their stability [20]. M. Soljačić et al demonstrated theoretically that the necklace-ring beam could be self-trapped and take on stable propagation characteristics in self-focusing Kerr media [17-21]. More recently, the dissipative spatial solitons induced by the external potentials have excited more and more attention, and the unique dynamic regimes of dissipative spatial solitons supported by sharp quasi-one dimensional(1D) potentials in the 1D and 2D-CGLE with CQ nonlinearity were investigated[22-34].For the conservative models, dissipative spatial solitons splitting by means of using an external potential in the 2D-CGLE with the "checkerboard" potential, has been reported [35]. In this paper, the spatiotemporal necklace-ring solitons in 3D-CGLE with the USP are investigated. Under the action of the appropriate USP, the vortices can evolve and form the spatiotemporal necklace-ring solitons. In addition, the formation of spatiotemporal necklace-ring solitons does not only depend on the USP but also transmission properties. These results are very helpful for understanding the formation and evolution of the spatiotemporal necklace-ring solitons completely and exploring many future potential applications.

2. The model

The propagation of an electromagnetic field u in the optical medium, which is described by the 3D-CQCGL equation [26,27]

$$i\frac{\partial u}{\partial z}+i\delta u+\left(\frac{1}{2}-i\beta\right)\left(\frac{\partial^2 u}{\partial x^2}+\frac{\partial^2 u}{\partial y^2}\right)+\left(\frac{D}{2}+i\gamma\right)\frac{\partial^2 u}{\partial t^2}+(1-i\varepsilon)|u|^2u-(\nu-i\mu)|u|^4u=F(x,y)u \tag{1}$$

where x, y and t denote the transverse coordinates and temporal coordinate, respectively, z represents the propagation distance. D(=1/2) denotes the anomalous dispersion propagation regime, ν is the quantic self-defocusing coefficient, δ is the coefficient corresponding to the linear loss (δ>0) or gain (δ<0),μ> 0 accounts for the quintic-loss parameter, and ε>0 is the cubic-gain coefficient, γ>0 accounts for spectral filtering in optics, β is the spatial-diffusion term, which appears in a model of laser cavities.

As a typical example, we concentrate on the USP [9,23], the analytical form of F(x,y) is

$$F(x,y) = -pr\left|\cos(m\theta)\right|^{\frac{1}{n}} \tag{2}$$

where $r=\sqrt{x^2+y^2}$,the parameter p denotes the depth of the potential; the parameter n determines the sharpness of the potential; θ is the angular coordinate, m stands for the number of folding umbrellas, as shown in Fig. 1(a).

The initial solutions of the vortex in Eq. (1) are expressed by

$$u(z=0,x,y,t) = A(x+iy)^S \exp\left[-\left(\frac{x^2+y^2}{w^2}+\frac{t^2}{w^2}\right)\right] \tag{3}$$

where A is the amplitude, S is the topological charge and w is the width. The stable vortices with S=1 and 2 are obtained, as shown in Figs. 1 (b) and (c). In this case, the 3D vortices with S=1 and 2 are all stable, characterized by the following values of the energy

$$E=\int_{-\infty}^{\infty}\int_{-\infty}^{\infty}\int_{-\infty}^{\infty}|u|^2\,dxdydt \tag{4}$$

and the average evolution radius

$$R=\int_{-\infty}^{\infty}\int_{-\infty}^{\infty}\int_{-\infty}^{\infty}\left(x^2+y^2\right)^{1/2}|u|^2\,dxdydt\Big/\int_{-\infty}^{\infty}\int_{-\infty}^{\infty}\int_{-\infty}^{\infty}|u|^2\,dxdydt \tag{5}$$

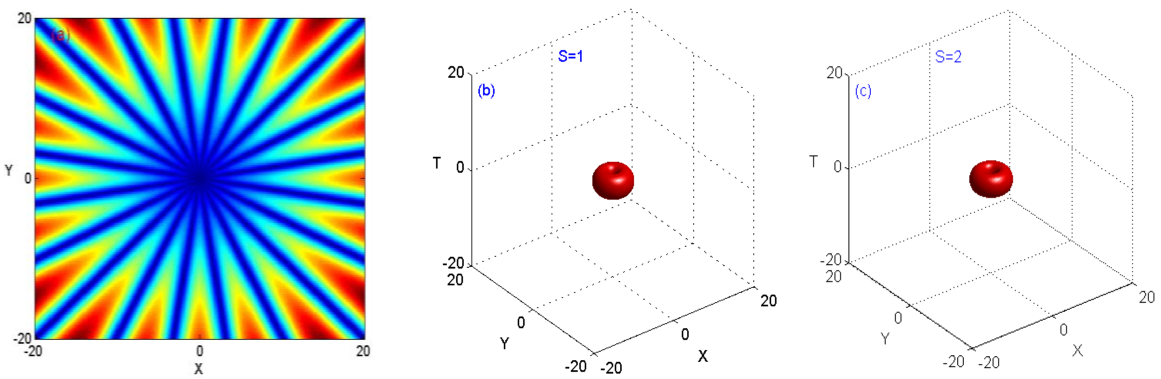

Fig. 1. (Color online) (a) Umbrella-shaped potential with p=1, n=1 and m=12. (b), (c) Intensity distribution of vortices with S=1 and S=2,respectively (color online)

3. Results and discussion

The numerical simulations are performed using the split-step Fourier method [36-37]. In simulations, we select the generic case for the set of parameters: $\delta=0.4$, $\mu=1$, $\varepsilon=2.43$, $\gamma=\beta=0.5$ and $\nu=0.1$. First, we analyze and discuss the generation and evolution properties of vortices with S=1 for different depth parameters p for other given parameters, namely, m=5, n=1 of the USP. Fig.2 shows the evolution of spatiotemporal NRSs with S=1 for different depths of the USP. When the depth parameter is 0.04, the vortices localize on the top of the potential, and the vortices gradually expand along the azimuthal direction with the increase of transmission distance, as shown in Fig. 2(a). The reason is because the potential is weak, the vortices localization is attributed to the viscous effect that prevents the vortices from splitting on the top of potential namely the vortices cannot form NRSs for the smaller and moderate depth. As the depth of the USP is increased to 0.07, the vortices will expand continuously on propagation distance from 0 to 60, and form annular beam at distance of 60; the vortices evolve NRSs as further increasing propagation distance, as shown in Fig. 2(b). As the depth of the USP equals to 0.09,the vortices expand continuously on propagation distance from 0 to 40, and form annular beam at distance of 40; the vortices evolve NRSs with further increasing propagation distance, as shown in Fig. 2(c).As the depth of the USP is increased to 0.12,the vortices expand continuously on propagation distance from 0 to 20, and form annular beam at distance of 20; the vortices evolve NRSs with further increasing the propagation distance, as shown in

Fig.2(d).These results show that the USP can provide a continuous source of energy necessary for the formation of NRSs, and that the stronger the potential is, the easier the division.

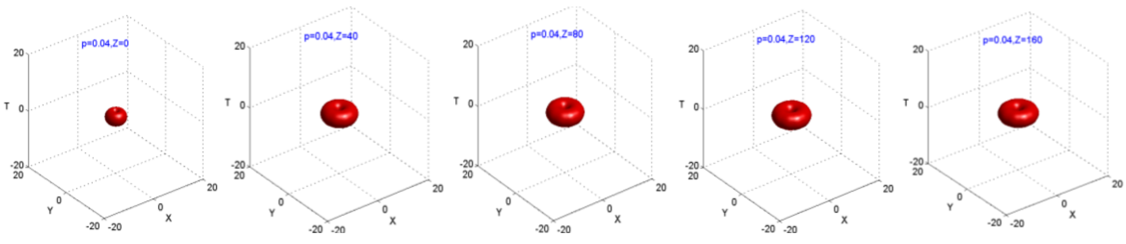

(a)

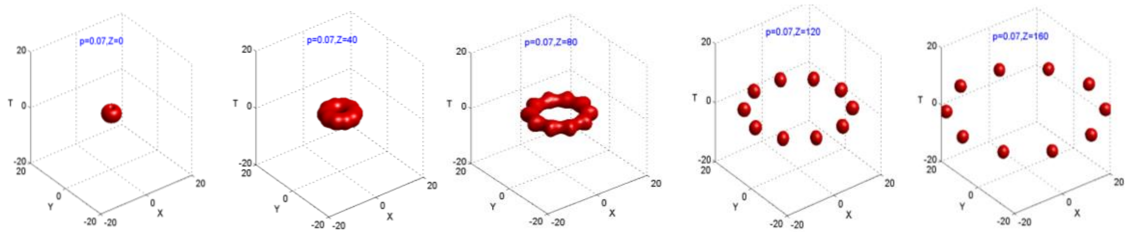

(b)

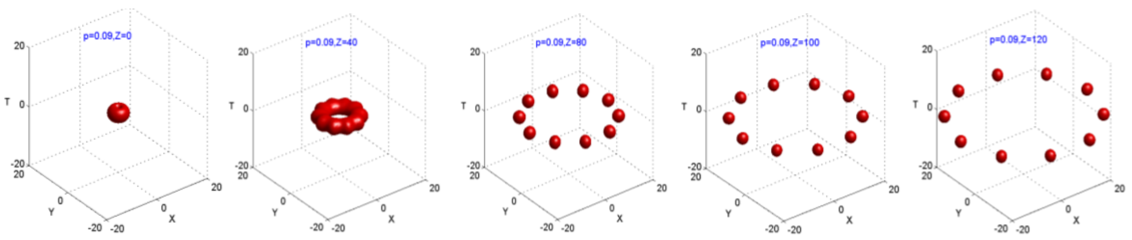

(c)

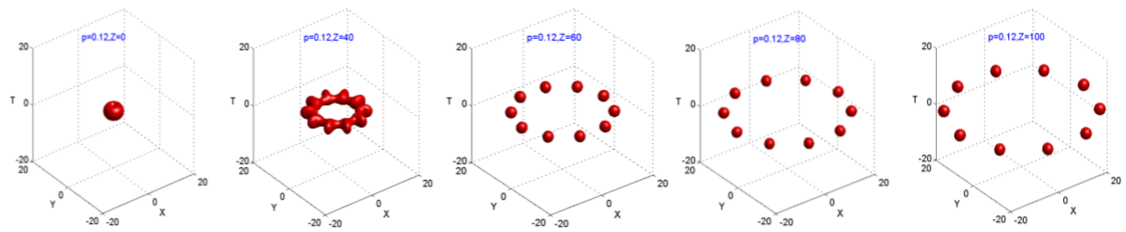

(d)

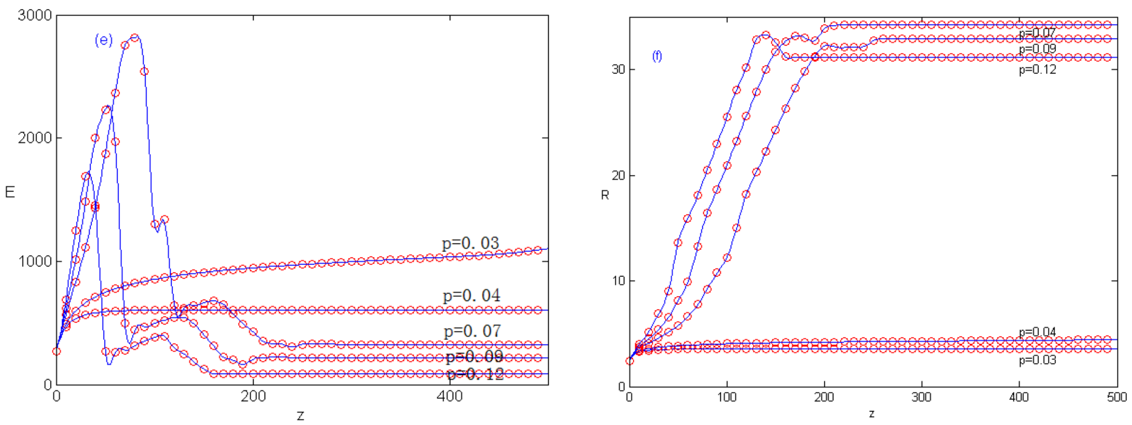

Fig. 2. (a)-(d) Isosurface plots of total intensity $|u(x,y,t)|^2$ *, evolutions of the central vortex with S=1 at (p=0.04, m=5), (p=0.07, m=5) (p=0.09, m=5), and (p=0.12, m=5). Evolutions of the energy of vortex with S=1 at m=5 with p=0.03, 0.04, 0.07, 0.09 and 0.12. (f) Evolutions of radius of vortex with S=1 at m=5 with p=0.03, 0.04, 0.07, 0.09 and 0.12 (color online)*

As the depth of the USP takes on strong enough, the vortices form NRSs on a certain distance. During propagation, the vortices gradually expand for the USP. The expanding velocity of the vortices depends on the sharpness, depth of the potential. As the depth of the USP increases, the push force becomes larger, and the vortices expand faster and form NRSs more easily. Fig. 2(e) presents the evolution of energy with different depths. Obviously, when the depths of the USP are 0.02 and 0.04,the energy gradually increases with increase of propagation distance, finally tends towards a steady state; As the depth parameters are increased to 0.07,0.09 and 0.12, the energy rapidly increases and reaches the maximum, then decreases with a sudden change and tends towards a steady state. The vortices decay and lose a large amount of energy. Fig. 2(f) presents the evolution radius for different depths. Obviously, when the depths of the USP are 0.03 and 0.04, the radius gradually increases with increase of propagation distance, finally tends towards a steady state. As the depth parameters are further increased to 0.07, 0.09 and 0.12, the radius rapidly increases and arrives at the maximum, then decreases with a sudden change and finally tends towards a steady state.

Fig. 3 presents the evolution of spatiotemporal NRSs with S=2 for different depths of the USP. Compared with Fig. 2(a), the vortices quickly evolve into annular beam at a shorter distance of 20, the annular beam continually enlarges with increase of propagation distance, however cannot form NRSs for the small and moderate depth, namely p=0.04, as shown in Fig. 3(a). As further increasing depth of the USP to 0.07, we can make clear that the vortices expand continuously, present necklace-like beam at propagation distance of 60 and form NRSs easily; NRSs can generate with increase of the propagation distance, as shown in Fig. 3(b). Obviously, as the depth of the USP is 0.09, the evolution and formation of NRSs are similarity with these in Fig. 2(c). As the depth of the USP is increased to 0.12, the vortices evolve NRSs immediately during propagation, as shown in Fig. 3(d). Fig. 3(e) presents the evolution of energy for different depths. Obviously, when the depths of the USP are 0.02 and 0.04, the energy gradually increases with increase of propagation distance, finally tends towards a steady state. As the depth parameters are increased to 0.07, 0.09 and 0.12, the energy rapidly increases and reaches the maximum, then decreases with a sudden change and arrive at a steady state. The vortices decay and lose a large amount of energy. Fig. 3(f) presents the evolution radius for different depths. Obviously, when the depths of the USP are 0.02 and 0.04, the radius gradually increases with increase of propagation distance, finally tends towards a steady state; as the depths are increased to 0.07,0.09 and 0.12, the radius rapidly increases, reaches the maximum, and then decrease with a sudden change and finally tends towards a steady state. Through above studies on the evolution of dissipative vortices with S=1 and 2, we find that the vortices with S=2 evolve into NRSs more early than these with S=1 for the same depth of the USP on a shorter propagation distance. As the depth of the USP becomes strong enough, the vortices form NRSs on a certain distance. The expanding velocity of the vortices depends on the sharpness, depth of the potential. As the depth of the USP increases, the push force becomes larger, therefore the vortices expand faster and easily form NRSs. By performing extensive numerical simulations, the potential is enough big, and the vortices do not form NRSs but decay more quickly.

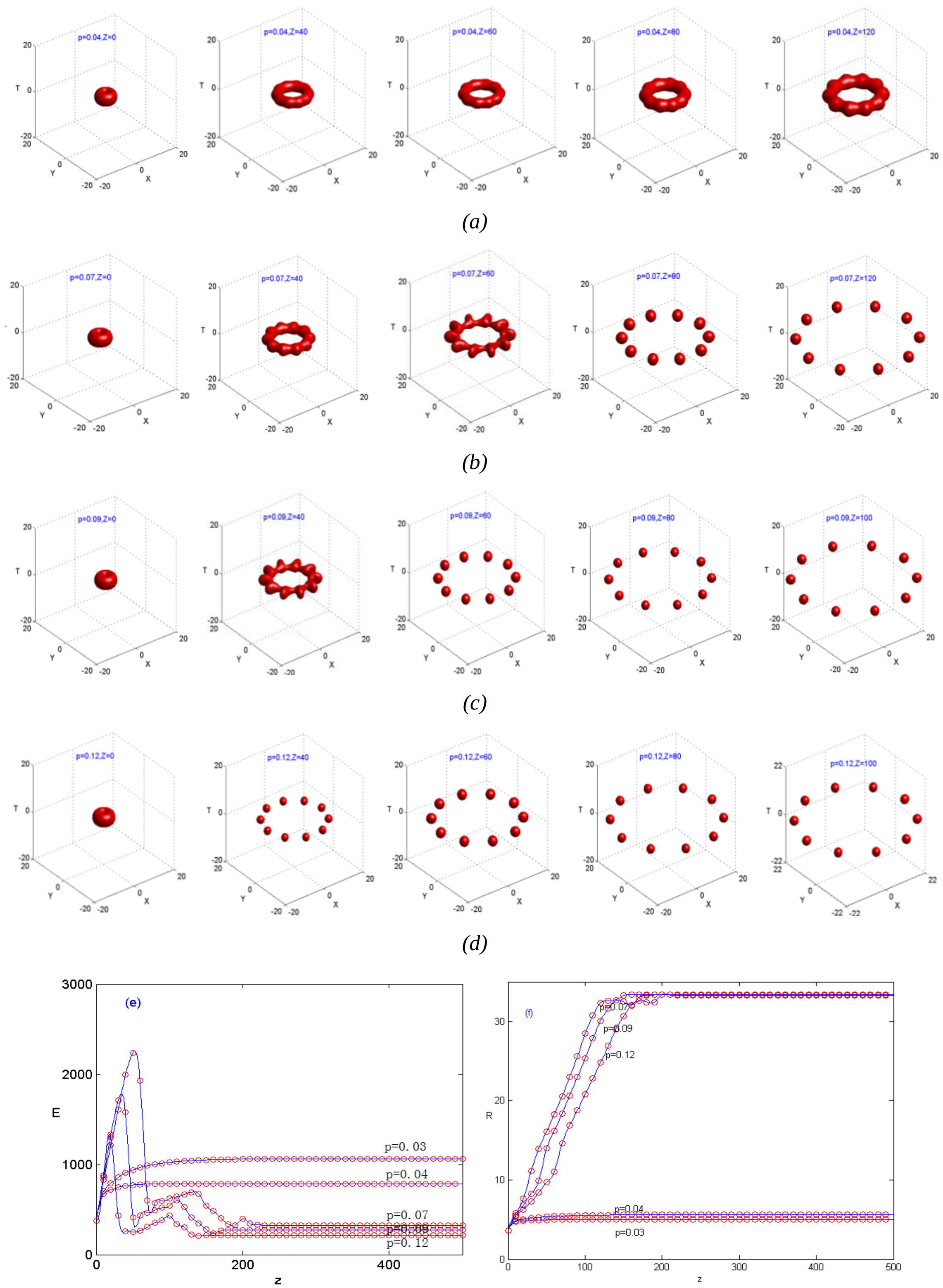

Fig. 3. (a)-(d) Isosurface plots of total intensity $|u(x,y,t)|^2$, evolutions of the central vortex with S=2 at (p=0.04, m=5), (p=0.07, m=5) (p=0.09, m=5), and (p=0.12, m=5). Evolutions of the energy of vortex with S=2 at m=5 with p=0.03, 0.04, 0.07, 0.09 and 0.12. (f) Evolutions of radius of vortex with S=2 at m=5 with p=0.03, 0.04, 0.07, 0.09 and 0.12 (color online)

4. Conclusions

In summary, the formation and evolution of spatiotemporal necklace-ring solitons induced by the USP are investigated comprehensively and thoroughly. The results show that the formation mechanism of spatiotemporal necklace-ring solitons does not only depend on the strength of the USP but also on different topological charges. For the appropriate potential, the vortices with the topological charges can evolve more easily spatiotemporal necklace-ring solitons on a certain propagation distance. However, lots of numerical simulations show that a strong potential will not make the vortices form NRSs, on the contrary the vortices collapse on a smaller propagation distance. These results suggest potential applications such as routing light signals, all-optical data-processing schemes in optical communication devices, dynamic and stationary ring-like beams in nonlinear dissipative media.

Acknowledgements

This work was supported by the National Natural Science Foundation of China (Nos.11864026 and 61661034),Jiangxi Provincial Department of Education Sc -ience and Technology Program(GJJ180536) and PhD research startup foundation of Nanchang Hangkong University (Grant No.EA201708388).

References

[1] S. Aranson, L.Kramer, Rev. Mod. Phys.**74**, 99 (2002).
[2] H. Li, Chin. Opt. Lett. **11**(s2), S21902 (2013).
[3] B. A. Malomed, Encycloperia of Nonlinear Science, Routledge, New York, p. 157, 2005.
[4] D. Mihalache, Rom. J. Phys. **59**, 295 (2014).
[5] L. L. Hao, C. F. Hou, Q.Wang, Chin. Opt. Lett. **12**, 041901 (2014).
[6] L. J. Ge, M. Shen, T. C. Zang, L. Dai, Chin. Opt. Lett. **12**, 121901 (2014).
[7] H. Li, Chin. Opt. Lett. 12(s1), S11904 (2014).
[8] G. Y. Jiang, Y. L. Liu, Chin. Opt. Lett. **13**, 041901 (2015).
[9] Y. F. Liu, B. Liu, X. D. He, S. J. Li, Chin. Phys. Lett. **31**, 074210 (2014).
[10] N. N. Rosanov, S. V. Fedorov, A. N. Shatsev, Lecture Notes in Physics **751**, 93 (2008).
[11] R. Kuszelewicz, S. Barbay, G. Tissoni, G. Almuneau, Eur. Phys. J. D **59**, 1 (2010).
[12] Y. J. He, B. A. Malomed, F. Ye, B. Hu. J. Opt. Soc. Am. B **27**, 1139 (2010).
[13] D. Mihalache, D. Mazilu, B. A. Malomed, F. Lederer, Phys. Rev. E **69**, 066614 (2004).
[14] D. Mihalache, D. Mazilu, F. Lederer, Phys. Rev. Lett. **97**, 073904 (2006).
[15] Y. J. He, H. H. Fan, J. W. Dong, H. Z. Wang, Phys. Rev. E **74**, 016611 (2006).
[16] S. V. Sazonov, Phys. Rev. A **100**, 043828 (2019).
[17] H. P. Zhu, L. R. Qian, Appl. Math. Lett. **82**, 118 (2018).
[18] S. V. Sazonov, M. S. Mamaikin, I. G. Zakharova et al., Phys. Wave Phenom. **25**, 83 (2017).
[19] S. V. Sazonov, M. S. Mamaikin, M. V. Komissarova et al., Phys. Rev. E. **96**, 022208 (2017).
[20] A. Barthelemy, C. Froehly, M. Shalaby, Proc. SPIE Int. Soe. Opt. Eng. **2041**, 104 (1993).
[21] M. Soljačić, S. Sears, M. Segev, Phys. Rev. Lett. **81**, 4851 (1998).
[22] M. Soljačić, M. Segev. Phys. Rev. E **62**, 2810 (2000).
[23] A. S. Desyatnikov, Yu. S. Kivshar, Phys. Rev. Lett. **87**, 033901 (2001).
[24] J. Yang, I. Makasyuk, H. Martin, Phys. Rev. Lett. **94**, 113902 (2005).
[25] B. Liu, Y. J. He, B. A. Malomed, Opt. Lett. **35**, 1974 (2010).
[26] Y. J. He, D. Mihalache, B. B. Hu, J. Opt. Soc. Am. B **27**, 2174 (2010).
[27] C. P. Yin, D. Mihalache, Y. J. He, J. Opt. Soc. Am. B **28**, 342 (2010).
[28] Y. J. He, B. A. Malomed, F. Ye, B. Hu, J. Opt. Soc. Am. B **27**, 1139 (2010).
[29] V. Skarka, N. B. Aleksic, H. Leblond, Phys. Rev. Lett. **105**, 213901 (2010).
[30] D. A. Zezulin, Y. V. Kartashov, V. V. Konotop, Opt. Lett. **36**, 1200 (2011).
[31] B. Liu, X. D. He, Opt. Exp. **19**, 20009 (2011).
[32] Y. J. He, D. Mihalache, J. Opt. Soc. Am. B **30**, 3135 (2013).
[33] B. Liu, X. D. He, S. J. Li, Opt. Exp. **21**, 5561 (2013).
[34] Y. J. He, B. A. Malomed, D. Mihalache, Phil. Trans. R. Soc. A **372**, 20140017 (2014).
[35] R. Driben, B. A. Malomed, A. Gubeskys, J. Zyss, Phys. Rev. E. **76**, 066604 (2007).
[36] M. Facao, M. I. Carvalho, Phys. Rev. E. **96**, 042220 (2017).
[37] G. P. Agrawal, Nonlinear Fiber Optics, 4^{th} ed., Academic Press, San Diego, USA, 2006.

*Corresponding author: jgy579@126.com